Hindawi
Mathematical Problems in Engineering
Volume 2024, Article ID 6037061, 11 pages
https://doi.org/10.1155/2024/6037061

Research Article

Quantitative Representation of Disturbance Waveform for Microgrid Connected PCC Voltages Using Improved Atomic Decomposition

Wenbo Hao,[1] **Jin Liu**,[1] **Qingyu Yan**,[2] **and Benran Hu**[2]

[1]*State Grid Heilongjiang Electric Power Research Institute, Harbin 150030, China*
[2]*State Grid Heilongjiang Electric Power Company Limited, Harbin 150000, China*

Correspondence should be addressed to Wenbo Hao; hwb150030@163.com

Received 3 September 2022; Revised 12 November 2023; Accepted 27 March 2024; Published 10 April 2024

Academic Editor: Ricardo Fabricio Escobar Jiménez

The fluctuation of microgrid power flow leads to serious voltage problems at the point of common coupling (PCC). The quantitative representation of the disturbance parameters of the voltage waveform at the PCC is necessary for evaluating and controlling the impact of distributed generation in the microgrid on the power system. An improved atomic decomposition (IAD) method is proposed to represent the disturbance parameters quantitatively and efficiently. Based on the disturbance characteristics of the PCC voltage, a coherent atom dictionary composed of four subdictionaries is constructed to improve the decomposition efficiency. To further improve the computational efficiency, an improved matching pursuits algorithm is proposed by alternating the search way to extract the disturbance components in the atomic decomposition. Meanwhile, simulation results show that the proposed IAD method has better antinoise and disturbance parameters quantization ability than wavelet transform.

1. Introduction

As the increased capacity of distributed generation in microgrids, power quality problems such as voltage deviation and fluctuation are more serious at the microgrid-connected point of common coupling (PCC) because of the fluctuation and intermittency of power flow [1]. The mitigating equipment, such as a static var compensator or static var generator, is usually installed at the PCC to improve the power quality. But whether and how much-mitigating equipment should be required to properly mitigate the power quality problem economically. The answer needs a sound evaluation of the PCC voltage influence by the microgrid. Evaluation of the historically recorded disturbance is an effective approach to estimating the PCC voltage influenced by the distributed power and decides whether mitigation is required. Generally, voltage profiles are expressed with root mean square (RMS) values. The recording interval may be one or several minutes. It is the average value of RMS in several cycles per recording data. This description can reflect only the steady-state voltage problems. Sometimes, we are concerned about the instantaneous voltage waveform caused by the fluctuation of distributed resources in microgrids, for example, the voltage sag waveform. In this circumstance, we need to record a piece of voltage disturbance waveform instead of presenting the RMS values. Due to the disturbances that exist all the time in microgrids; therefore, the recorded waveform is tremendous. If the waveform is stored and transmitted in the form of sampling data, the dimension is huge and hard to deal with. If the data are modeled properly and only the modeling parameters are stored and transmitted, the data dimension will be reduced greatly [2–4].

At present, many experts have done a lot of research on the analysis and detection of interference signals [5]. By analyzing the recovery and reconstruction process of various power-quality single disturbances and composite disturbance signals, a set of acquisition methods suitable for power-quality disturbance (PQD) signals was proposed in [6]. Long-term gapless oscillographic analysis was proposed in [7] for efficient real-time compression of data. Chen et al. [8] proposed several methods to compress the synchrophasor and POW data in a lossless manner. Literature [9] proposed a singular

value decomposition-based method for the compression of synchrophasor data, which provided high CR and preserved the critical information of events and disturbances. In [10], considering the patterns, potential applications, and associated precision to preprocess the time series, the lossless coding considering the precision method was proposed.

Signal model parameter extraction methods based on wavelet transform (WT) or analysis methods combined with other methods are widely used [11–13]. In this method, the disturbance signal is decomposed first, and then the residual coefficient and detail coefficient of each scale are applied to a certain threshold to compress the feature data. In [11], a wavelet denoising method based on variational mode decomposition and multiscale permutation entropy was proposed to analyze vibration fault characteristics. Literature [12] presented a methodology to characterize voltage sags using fault analysis and deep convolutional neural networks, and the discrete WT was used in signal processing. In [13], to separate the interharmonic components, a set of new scaling filters and wavelet filters with narrow transition bands was designed for the undecimated wavelet packet transform.

Overall analysis, WT has good time–frequency domain localization characteristics, which can provide the characteristics of disturbance signals at different scales, but it is vulnerable to noise and has poor application effect on low-frequency disturbances such as voltage sag and voltage swell. Therefore, these methods cannot obtain the accurate model parameters of the disturbance signals.

Atomic decomposition algorithm technology has been a hot research topic in the field of signal processing in recent years. This method originates from the idea proposed by Mallat and Zhang to decompose signals on overly complete non-orthogonal bases [14]. The atomic decomposition method decomposes signals based on an over-complete dictionary, which can improve the sparse representation of signals [15]. Sparse signal representation has good adaptability and high flexibility in describing any complex signal based on atomic decomposition, which is not limited by an orthogonal basis. It provides an effective method for extracting features from complex signals for fault diagnosis [16]. Tcheou et al. [17] analyze the problem of using atomic decompositions for rate-distortion-optimum compression of signals from electric power system disturbances. They use different dictionaries corresponding to different quantizers of atomic parameters. These quantizers can provide near-optimum rate-distortion performance. Gao et al. [18] propose an internal overvoltage identification method based on time–frequency atomic decomposition, which mainly decomposes the overvoltage waveform using the atomic decomposition algorithm and obtains effective atoms from the waveform. Then, by combining corresponding recognition standards, the hierarchical identification of overvoltage types is achieved. The experimental results show that the algorithm has high accuracy and strong adaptability.

However, traditional atomic decomposition algorithms used for PQD signals have problems with excessive computational resource consumption and low subdictionary selection accuracy. The conventional atomic decomposition algorithm for PQD signals is optimized by introducing a convolutional neural networks-based subdictionary predictor inspired by the PQD signal classification technique [19]. They verify that this method can reduce the demand for computing resources and improve the accuracy of subdictionary selection in signal decomposition. To accurately extract fault features from noise signals, Zhang et al. [20] propose an improved orthogonal matching pursuit (MP) with an adaptive Gabor subdictionary. It can significantly improve the efficiency of signal sparse representation while ensuring accuracy. Agarwal et al. [21] present a novel algorithm for the estimation of overcomplete dictionaries. Under the probabilistic model of generating data as well as assumptions on the coefficients and dictionaries, it can be guaranteed that such a procedure approximately recovers the unknown overcomplete dictionary.

In this paper, we proposed an improved atomic decomposition (IAD) method to model the voltage disturbances in microgrids. The contribution of this work is as follows:

(1) An efficient disturbance modeling method based on atomic decomposition is presented to extract the model parameters.
(2) An improved MP algorithm is proposed to decrease computation quantities by alternating the search way of selecting the optimal atoms.
(3) The coherent atom dictionary is constructed according to the characteristics of the PCC voltage disturbance to improve the decomposition efficiency.

After the introduction, the principle of atomic decomposition, as well as the expression method for disturbances with atoms, is discussed in Section 2. Section 3 discusses the construction of the coherent atom dictionary and the improved MP algorithm. In Section 4, the performance of the proposed IAD method is evaluated with simulations. Finally, the conclusions are listed in Section 5.

2. Modeling of Signals with Atoms

2.1. Principle of Atomic Decomposition. Dictionary D is defined as a set of all possible basic items representing the signal waveforms. In this paper, the signals are voltage disturbances collected at the PCC of microgrids. D is called a dictionary of atoms. The ideal signal $\widehat{X}$ can be represented by the linear combination of elements $g_{\gamma(m)}$ selected in D.

$$\begin{cases} X = \sum_{m=1}^{n} \alpha_m g_{\gamma(m)} + \gamma_X^m \\ \widehat{X} = \sum_{m=1}^{n} \alpha_m g_{\gamma(m)} \end{cases}, \; g_{\gamma(m)} \in D, \tag{1}$$

where $g_{\gamma(m)}$ is the atoms of dictionary D, and $\gamma(m)$ is an indexing parameter associated with a particular dictionary element in D. α_m is the amplitude of atom $g_{\gamma(m)}$, $m = 1, 2, \ldots, n$, and n is the number of atoms. In neglecting the residual parts, the analyzed signal X is approximately equal to $\widehat{X}$. Therefore, the practical signal X can be expressed approximately by the combination of $g_{\gamma(m)}$.

Usually, the dictionary D is over-complete to ensure that any signal can be represented by an optimal set of elements selected adaptively, resulting in the sparsity of the expression. Atomic decomposition differs from other signal transformations, for it permits the linear dependency among the selected atoms. Because the decomposition in the over-complete dictionary is not unique, it permits the selection with different atoms to compose X, therefore, leading to sparse and compact representation. For a specific signal, the best expansion function can be selected adaptively from an over-complete set of expansion functions according to the signal characteristics. Such expansion functions are more accurate to represent the signal. The expanded functions in the over-complete set are atoms, and the over-complete set composed of atoms is called the atomic dictionary. Atoms are generated by stretching, translating, and modulating from a window function $g(t)$.

The key issue in atomic decomposition is how to search the energy factor α_m and the atom $g_{\gamma(m)}$. Here, we accomplish the search by using the MP algorithm described in Section 2.2. The atoms in the dictionary are usually obtained by scaling, transforming, and modulating some special functions. One of the common methods is to use Gabor as the mother function to form the Gabor atoms, as shown in Equation (2).

$$g_\gamma(t) = \frac{K_\gamma}{\sqrt{s}} g\left(\frac{t-\tau}{s}\right)\cos(\xi t + \phi), \tag{2}$$

where $g(t) = 2^{\frac{1}{4}}e^{-\pi t^2}$ is the Gaussian window, $\gamma = (s, \tau, \xi, \phi)$ is the parameter group of atoms, s is the scale factor, τ is the translation factor, ξ is the frequency modulation factor, and ϕ is the phase. The phase $\phi \in [0, \pi)$ and K_γ is assigned to make $\|g_\gamma(t)\| = 1$.

Theoretically, the denser the atom distributions in the dictionary get, the more concise the signals are represented, while the dictionary gets larger. The overlarge dictionary is adverse to computation. It is impossible to search in a dictionary with infinite atoms. Therefore, parameters of the atoms should be discrete sampled to obtain a finite while redundant dictionary. The discretization of atom parameters obeys that $\gamma = (2^j, 2^j p, 2^{1-j}k\pi, \phi)$, where $j, p, k \in Z$ are the integers, $\phi \in R$ is a real number. Thus, γ can be uniquely represented in discrete form as $\gamma_s = (j, p, k, \phi) \in Z^3 \times R$, where j dominates the atom scaling, p dominates time shift, and k dominates the atom modulation. Let the length of the signal is N, then the atoms in the finite discrete dictionary are expressed as follows:

$$g_{rd}(n) = g_j(n - p2^j)\cos(nk\pi 2^{1-j} + \phi) n = 0, 1, \ldots, N-1$$
$$g_j(n) = \begin{cases} \delta(j) & j = 0 \\ K_{\gamma d} g(n2^{-j}) & j \in [1, L) \\ \dfrac{1}{\sqrt{N}} & j = L \end{cases}, \tag{3}$$

where $L = \log_2 N, j \in [0, L], p \in [0, 2^{-j}N], k \in [0, 2^j)$. The phase parameter ϕ is unnecessary to be searched separately; it can be derived from parameters $[s, \tau, \xi]$ depicted in [22].

2.2. MP Algorithm. Implementation of atomic decomposition directly through optimization is a hard problem. As a suboptimal scheme, the MP algorithm is usually used in the atomic decomposition [18]. MP algorithm is a greedy iterative algorithm. In each iteration, the atom that best matches the signal or the residual component of the signal is extracted from the atomic dictionary. The signal is represented as a linear combination of the best-matched atoms. The number of iterations or the energy of the residual signal is restricted as the end condition of the decomposition.

Suppose the signal to be analyzed is $f, f \in H$, H is a finite-dimensional Hilbert space. D is an over-complete atomic dictionary, $D \in H$, g_γ is an atom of D, γ is the atomic parameter group, Γ is the set of parameter groups, $\gamma \in \Gamma$. The atoms are usually normalized, that is, $\|g_\gamma\| = 1$. First, select the atom $g_{\gamma(0)}$ from D that best matches the signal f, and the $g_{\gamma(0)}$ satisfy as follows:

$$\left|\left\langle f, g_{\gamma(0)}\right\rangle\right| = \max_{\gamma\in\Gamma}\left|\left\langle f, g_\gamma\right\rangle\right|. \tag{4}$$

Equation (4) $\langle , \rangle$ represents the inner product of the two quantities. Signal f is divided into two parts: the component on the optimal atom $g_{\gamma(0)}g_{\gamma(0)}$ and the residual component, namely,

$$f = \left\langle f, g_{\gamma(0)}\right\rangle g_{\gamma(0)} + r_f^1, \tag{5}$$

where r_f^1 is the residual component after the 1st atomic decomposition of signal f. The residual components will be further extracted to gain more atomic components. The iteration is as follows:

$$r_f^m = \left\langle r_f^m, g_{\gamma(m)}\right\rangle g_{\gamma(m)} + r_f^{m+1}, \tag{6}$$

$g_{\gamma(m)}$ satisfy as follows:

$$\left|\left\langle r_f^m, g_{\gamma(m)}\right\rangle\right| = \max_{\gamma\in\Gamma}\left|\left\langle r_f^m, g_\gamma\right\rangle\right|. \tag{7}$$

After n iterations, let the residual component is r_f^n, then the signal f can be expressed as follows:

$$f = \sum_{m=1}^{n-1}\left\langle r_f^m, g_{\gamma(m)}\right\rangle g_{\gamma(m)} + r_f^n. \tag{8}$$

Therefore, through n iterations, signal f can be represented by a linear combination of n atoms, adding the error. The error is the residual component after n iterations. In discrete forms, if the length of the signal is finite and n increases infinitely, the $\|r_f^n\|$ decays exponentially to zero. In general, the main components of the signal can be represented very sparse by the atoms compared to the signal length.

3. Improvement of Atom Decomposition

3.1. Construction of Damped Sinusoidal Coherent Atoms. The voltage disturbances in microgrids connected to PCC are mainly the fundamental component. According to the principle of atomic decomposition, if the atoms have similar structures to the analyzed signal, the performances of atomic decomposition, such as the efficiency and the accuracy will get better. This kind of atomic dictionary is specially constructed for a certain type of signal and is called the coherent atom dictionary [21]. In this paper, we employ damped sinusoidal atoms to build the coherent atom dictionary instead of using the Gabor dictionary. The other reason for introducing damped sinusoidal atoms to substitute Gabor atoms is that the parameters of Gabor atoms have no physical significance. This is a disadvantage to evaluating the disturbances.

The expression of the signal with damped sinusoidal atoms is shown in Equation (9).

$$f(t) = \sum_{q=0}^{Q-1} A_q \cos\left(2\pi f_q t + \phi_q\right) e^{-\rho_q\left(t-t_{sq}\right)} \times \left[u\left(t-t_{sq}\right) - u\left(t-t_{eq}\right)\right], \tag{9}$$

where A_q is the amplitude of damped sinusoidal atoms, f_q is the frequency, ρ_q is the damping factor, ϕ_q is the phase, $u(t)$ is the unit step function, t_{sq} and t_{eq} are the component starting and ending time, respectively.

The key issue of this dictionary is that the discrete atom parameter group $(A_q, f_q, \rho_q, \phi_q, t_{sq}, t_{eq})$ of Equation (9) needs to be determined. Here, we use Gabor atoms to produce the damped sinusoidal atoms. The procedure is shown in Figure 1.

Step 1. Decompose the signal in the Gabor dictionary with the MP algorithm to acquire parameters $[s,\ \xi, u]$.

Step 2. Deduce approximately the damped sinusoidal atoms from Gabor ones obeying the steps as follows:

(1) Determine the position of the greatest inner product of Gabor atoms and the signal or residuals. If the position lies on the right-hand of the center τ of the Gauss window function, the sinusoidal atoms are attenuated. Otherwise, if the position lies on the left-hand, the sinusoidal atoms are divergent.

(2) Calculate the initial estimated value of the damped coefficient ρ based on the time scale s. If the sinusoidal atoms are attenuated, $\rho = \sqrt{\pi/2s^3}$. On the contrary, if the sinusoidal atoms are divergent, $\rho = -\sqrt{\pi/2s^3}$. Such a treatment can maintain the equivalence between the damped sinusoidal atom and the Gabor atom in the central point τ. Note that ρ is not the ultimate value; it should be optimized latterly.

(3) The starting and ending times of the sinusoidal atom were obtained using the method as [22].

Step 3. Optimize the parameters to acquire the ultimate sinusoidal atoms. Here, the Pseudo-Newton algorithm is occupied. The detailed processes are as follows:

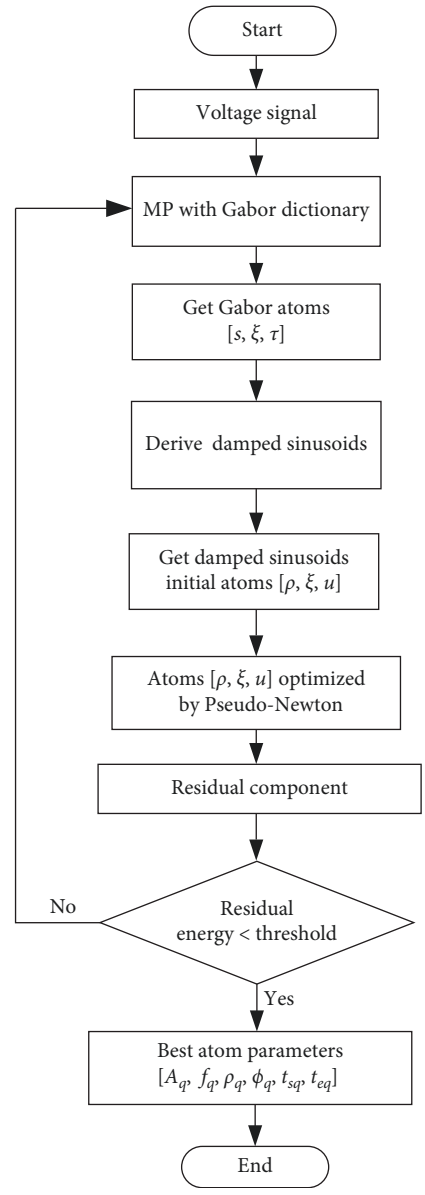

FIGURE 1: The procedure of solving damped sinusoidal atoms parameters based on MP.

(1) Increment the parameters $[\rho, \xi, u]$ in turn. The incremental quantities are assigned to half the parameter values.

(2) Build atoms based on the newly created parameters and obtain the inner products for each atom with the residual of the approximate damped sinusoidal atoms. If one of the products is increased, then substitute the original atom with the new one and continue the next judgment. Otherwise, reduce the incremental value of the atom parameters by 1/4 and continue searching.

(3) If the incremental quantity of the product is lower than a given threshold, then terminate the current optimizing process and optimization for the next parameter.

Through optimizations, the discrete parameters of atoms tend to be denser. The over-complete characteristics are ensured. The complex forms of Gabor atoms are advantageous to real signals in practice that the phases are unconsidered temporarily. After $[s,\ \xi, u]$ are determined, the phase can be derived from them. This will simplify the computation greatly.

3.2. Categories of Atoms in the Coherent Dictionary. As discussed above, the atoms are permitted to construct according to the characteristics of the specific signal. The algorithm is presented to produce damped sinusoidal atoms from Gabor. Damped sinusoidal atoms are more suitable for voltage disturbances of microgrids connected to PCCs. Considering the possible behavior of voltage disturbances, we construct different categories of detail subdictionaries to suit for different behaviors of disturbances such as voltage sags, voltage surges, voltage interruptions, and so on. The categories of subdictionaries are mentioned in the following sections.

3.2.1. Fundamental Subdictionary of Atoms. The fundamental component is usually the most predominant one in the disturbances. The fundamental subdictionary of atoms is constructed, as shown in Equation (10).

$$g_{1\gamma_1}(t) = K_{\gamma_1}\cos(\omega_1 t + \phi_1), \tag{10}$$

where $\gamma_1 = [\omega_1, \phi_1]$, ω_1 is the angular frequency of the fundamental component, ϕ_1 is the phase, and K_{γ_1} is the coefficient that makes $\|g_{1\gamma_1}(t)\| = 1$. The length of signal $f(t)$ is N, then the parameters are discretized as $\gamma_1 = [2\pi j/N, 2\pi p/N]$, $j \in [1, N]$, $p \in [0, N-1]$.

Let the sampling rate of the signal $f(t)$ be f_s, the relationship between the frequency f of the signal $f(t)$ and discrete angular frequency ω is as follows:

$$f = f_s\omega/(2\pi). \tag{11}$$

Let $g^1_{1\gamma_1}(t) = \cos(\omega_1 t + \phi_1)$, then Equation (10) can be written as follows:

$$g_{1\gamma_1}(t) = K_{\gamma_1} g^1_{1\gamma_1}(t). \tag{12}$$

Then

$$K_{\gamma_1} = 1/\sqrt{\left\langle g^1_{1\gamma_1}(t), g^1_{1\gamma_1}(t)\right\rangle}. \tag{13}$$

According to the MP algorithm, a best-matching atom $g_{1\gamma_1}(t)$ can always be found. Let the best matching parameters ω and ϕ of the fundamental component are ω_1 and ϕ_1, and the sinusoid is expressed with $f_1(t)$, then

$$f_1(t) = A g^1_{1\gamma_1}(t), \tag{14}$$

where A is the amplitude of the fundamental component $f_1(t)$.

According to Equation (5),

$$f_1(t) = \left\langle f(t), g_{1\gamma_1}(t)\right\rangle g_{1\gamma_1}(t). \tag{15}$$

Substitute Equations (12) and (14) into Equation (15) to obtain Equation (16).

$$A = K_{\gamma_1}\left\langle f(t), g_{1\gamma_1}(t)\right\rangle. \tag{16}$$

3.2.2. Fundamental-Like Subdictionary of Atoms. For voltage disturbances such as voltage sag, voltage rise, and voltage interruption, their frequencies are still the fundamental frequency, but their phases are altered. Here, voltage sag, voltage rise, and voltage interruption are referred to as fundamental-like disturbances. The fundamental-like subdictionary of atoms is shown in Equation (17).

$$g_{2\gamma_2}(t) = K_{\gamma_2}\cos(\omega_1 t + \phi_2)\left[u\left(t - t_{s_2}\right) - u\left(t - t_{e_2}\right)\right], \tag{17}$$

where ω_1 is the angular frequency of the fundamental component obtained by the MP algorithm, $\gamma_2 = [\phi_2, t_{s_2}, t_{e_2}]$, ϕ_2 is the phase of the fundamental-like disturbance, t_{s_2} and t_{e_2} are the starting time and ending time of the fundamental-like disturbance, respectively, K_{γ_2} is the coefficient that makes $\|g_{2\gamma_2}(t)\| = 1$, $u(t)$ is the unit step function.

When the fundamental-like disturbance is in phase with the fundamental component, the disturbance is a voltage rise; when the fundamental-like disturbance is in opposite phase with the fundamental component, it is a voltage sag or interruption. Otherwise, it is a voltage transient. The parameters are discretized as $\gamma_2 = [2\pi q/N, n_{s_2}, n_{e_2}]$, $q \in [0, N-1]$, $0 \le n_{s_2} < n_{e_2} \le N-1$. The MP algorithm can still be used to extract the fundamental-like disturbance. The amplitudes can be obtained by substituting Equation (16) with the parameters. The start time t_s and end time t_e with the discrete start point n_s and end point n_e are as follows:

$$t_s = n_s/f_s, \tag{18}$$

$$t_e = n_e/f_s. \tag{19}$$

3.2.3. Pulse Atomic Dictionary. The voltage notch and voltage spike disturbances with short duration are referred to as pulse disturbances. The pulse subdictionary of atom is shown in Equation (20).

$$g_{3\gamma_3}(t) = K_{\gamma_3}\left[u\left(t - t_{s_3}\right) - u\left(t - t_{e_3}\right)\right], \tag{20}$$

where $\gamma_3 = [t_{s_3}, t_{e_3}]$, t_{s_3} and t_{e_3} are, respectively, the start time and end time of the pulse disturbance, and K_{γ_3} is the coefficient to make $\|g_{3\gamma_3}(t)\| = 1$. Pulse disturbances are also extracted through the MP algorithm. Their amplitudes can

be obtained by substituting Equation (16) with the parameters. As the pulse atoms in the subdictionary are expressed in positive, they are voltage spikes when the best-matched maximum inner product is positive. Otherwise, they are voltage notches when the best-matched maximum inner product is negative. It is generally believed that the duration of a voltage notch or voltage spike is less than 1/4 fundamental cycle. Therefore, the parameters can be discretized as $\gamma_3 = [n_{s_3}, n_{e_3}]$, $0 \le n_{s_3} < n_{e_3} \le N-1$, and $0 \le n_{e_3} - n_{s_3} \le f_s/(4f)$.

3.2.4. Oscillatory Subdictionary of Atoms. Voltage disturbances such as voltage harmonics, interharmonics, attenuated oscillations, and divergent oscillations are referred to as oscillatory disturbances. Oscillatory atoms are shown in Equation (21).

$$g_{4\gamma_4}(t) = K_{\gamma_4}\cos(\omega_4 t + \phi_4)e^{-\rho_4(t-t_{s_4})}\left[u(t-t_{s_4}) - u(t-t_{e_4})\right], \tag{21}$$

where $\gamma_4 = [\omega_4, \phi_4, \rho_4, t_{s_4}, t_{e_4}]$, ω_4 is the angular frequency of the oscillation, ϕ_4 is the phase, ρ_4 is the attenuation coefficient, t_{s_4} and t_{e_4} are the start time and end time, respectively, K_{γ_4} is the coefficient to make $\|g_{4\gamma_4}(t)\| = 1$. If $\rho_4 = 0$, the oscillatory disturbance is harmonic or interharmonic; if $\rho_4 > 0$, the oscillatory disturbance is the attenuated oscillatory disturbance; and if $\rho_4 < 0$, the oscillatory disturbance is a divergent oscillatory disturbance. The oscillatory disturbances can be extracted through the MP algorithm as well. Their amplitudes can be obtained by substituting Equation (16) with the parameters. The discretized parameters are as $\gamma_4 = [2\pi w/N, 2\pi s/N, m/N, n_{s_4}, n_{e_4}]$, $w \in [1, N]$, $s \in [0, N-1]$, $m \in [-N, N]$, $0 \le n_{s_4} < n_{e_4} \le N-1$. The relationship between the attenuation coefficient ρ and the discrete attenuation coefficient ρ' is as follows:

$$\rho = \rho' f_s. \tag{22}$$

Among the four coherent subdictionaries, the fundamental subdictionary and the fundamental-like subdictionary are attributed to the oscillatory subdictionary in essence. They are listed separately mainly to reduce the computation and improve the accuracy of signal extraction. If the fundamental subdictionary is triggered merely, only two parameters are searched in the iteration. If the fundamental-like subdictionary is triggered, three parameters should be searched in the iteration. If the oscillatory subdictionary is triggered, five parameters should be searched. When the abovementioned atoms are used in turn, the computation will be reduced greatly. The fundamental component in the signal is extracted first by the fundamental atoms to remove the best-known component. Then, the residual components are extracted by the other atoms.

3.3. Improvement of MP Algorithm. To reduce the amount of computation further, the MP algorithm is improved by searching the parameters step by step and searching manners from rough to fine. The following takes the MP algorithm in the fundamental-like atoms as an example.

For $\gamma_2 = [\phi_2, n_{s_2}, n_{e_2}]$, a step-by-step search is taken for ϕ_2, n_{s_2} and n_{e_2}. First, search ϕ_2 and n_{s_2} at the same time, and implement rough search first and fine search second for both ϕ_2 and n_{s_2}. The procedure is, dividing the sampling points N into M equal parts, let $\phi'_2 = 2\pi i/M$ ($i \in [0, M-1]$, $0 \le n'_{s_2} \le M-1$) to calculate with MP and get the rough matching parameters $\phi'_{2\lambda}$ and $n'_{s_2\alpha}$ ($\lambda \in [0, M-1]$, $\alpha \in [0, M-1]$). Search for $(2N/M-1)$ times by step $2\pi/N$ in the range $[\phi'_{2\lambda} - 2\pi(N/M-1)/N, \phi'_{2\lambda} + 2\pi(N/M-1)/N]$ in fine search to obtain the best matching parameter ϕ_{2r} ($r \in [0, N-1]$). Similarly, search for $(2N/M-1)$ times in the range $[n'_{s_2\alpha} - (N/M-1), n'_{s_2\alpha} + (N/M-1)]$ to obtain the best matching parameter $n_{s_2\beta}$ ($\beta \in [0, N-1]$). For n_{e_2}, it is obliviously after n_{s_2}. In case that n_{s_2} has been acquired, n_{e_2} will be in the interval of $[n_{s_2\beta}, N-1]$, the searching interval is reduced. Therefore, the best matching parameter $n_{e_2\theta}$ ($\theta \in [0, N-1]$) needs to be searched in the interval of $[n_{s_2\beta}, N-1]$ merely. The computational complexity is downgraded. Through improvement of the MP algorithm, the computational complexity is $[M^2 + (2N/M-1)^2] + (N - n_{s_2\beta})$, while the computational complexity using the direct MP algorithm is $N^2(N-1)/2$. If N is 1,024 points and M is 128, the computational complexity of the direct MP algorithm is 536346624. The computational complexity of the presented MP algorithm is $(17\,633 - n_{s_2\beta})$, which is downgraded greatly.

The orders to search the parameters are different also for different components. For the fundamental component, ω_1 should be searched first and then ϕ_1. For the impulsive disturbances, n_{s_3} and n_{e_3} should be searched simultaneously. For the oscillatory disturbances, the orders are ω_4 is searched first, and ϕ_4 and n_{s_4} is simultaneously searched following, then ρ_4 is searched, n_{e_4} is searched finally. In each step, the parameters are searched from rough to fine.

4. Case Studies

The proposed modeling method is applied to microgrids connected disturbance signals. The sampling frequency is 3,200 Hz, the fundamental frequency is 50 Hz, and the sampling signal length is 1,024 points. The performance of the proposed IAD method is evaluated by the modeling efficiency E_m, normalized mean-square error N_{MSE} and energy ratio N_{power}, respectively. The definition of each indicator is as follows:

$$E_m = \frac{L_a}{L_s}, \tag{23}$$

$$N_{\mathrm{MSE}} = \frac{\left\| f(n) - \widetilde{f}(n) \right\|^2}{\|f(n)\|^2}, \tag{24}$$

$$N_{\mathrm{power}} = \frac{\left\| \widetilde{f}(n) \right\|^2}{\|f(n)\|^2}, \tag{25}$$

where L_a is the number of parameters of the total atoms to represent the signal, L_s is the length of the original signal,

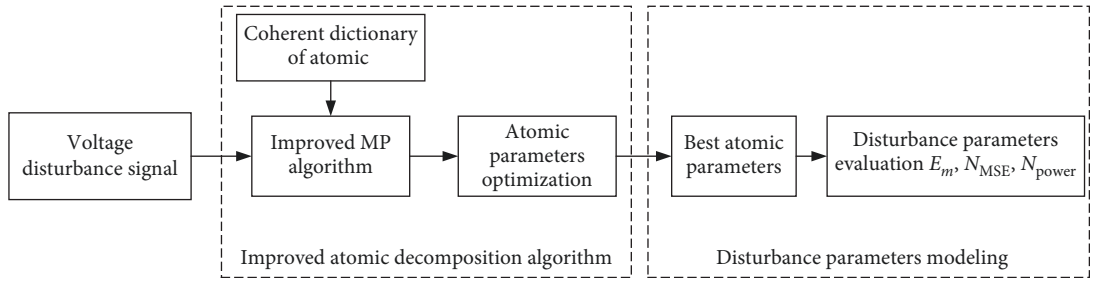

FIGURE 2: The schematic diagram of disturbance parameter modeling based on improved atomic decomposition.

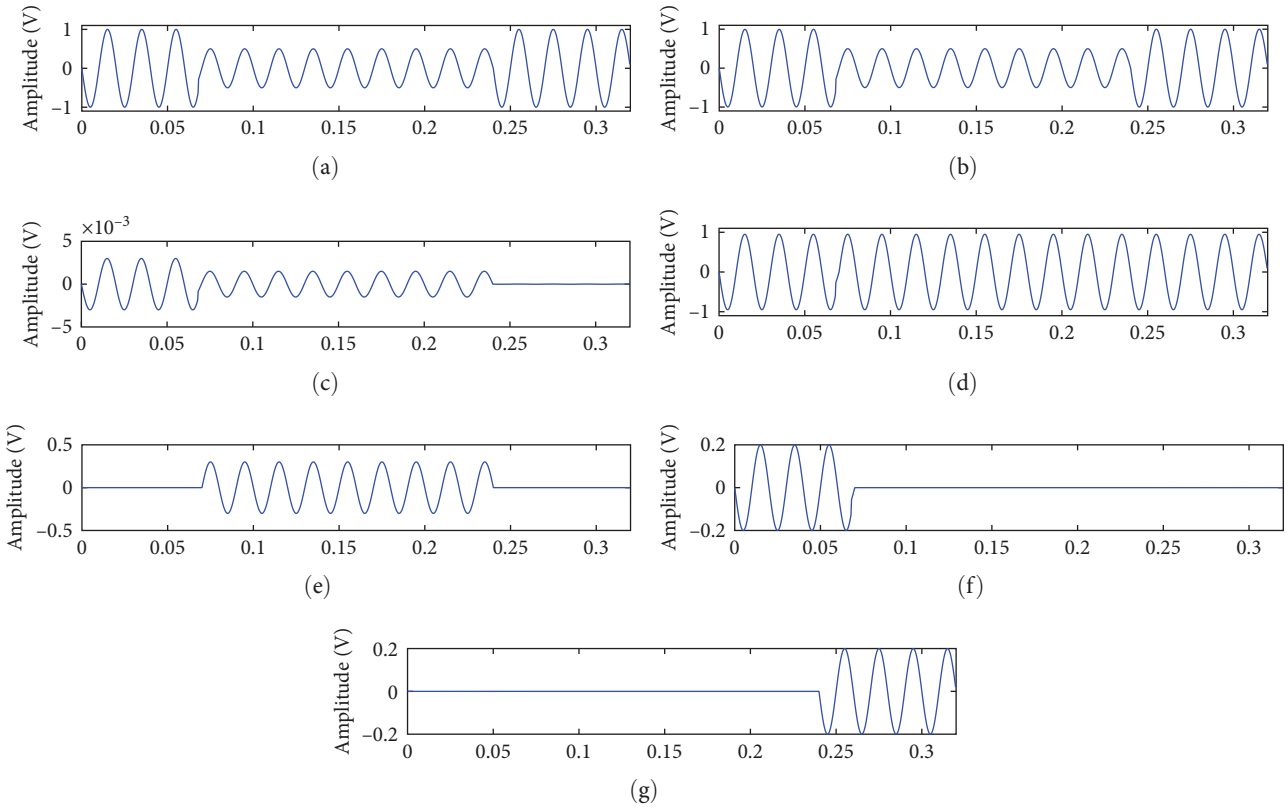

FIGURE 3: Decomposition results of IAD for voltage sag signal: (a) the original sag signal; (b) the reconstructed signal; (c) the residual component; (d) the first atomic component; (e) the second atomic component; (f) the third atomic component; (g) the fourth atomic component.

$f(n)$ is the original signal, and $\tilde{f}(n)$ is the reconstructed signal with atom decomposition.

Figure 2 shows the schematic diagram of disturbance parameter modeling based on IAD. The IAD algorithm is used to decompose several typical voltage disturbance signals at the microgrid-connected PCC. Then, the voltage disturbance parameters are determined based on the best atomic parameters, and the performance of the proposed method is evaluated through evaluation indicators E_m, N_{MSE}, N_{power}.

4.1. Voltage Sag. Figure 3(a) shows the original voltage sag signal with a 50% drop, which was decomposed by the IAD method with only four iterations to obtain the atoms' components, as shown in Figure 3(d)–3(g), and the parameters are listed in Table 1. The reconstructed signal and residual are shown in Figures 3(b) and 3(c), respectively. As can be seen from Figure 3 and Table 1, the fundamental component and voltage sag disturbance component in the signal can be extracted using the atomic library and matching tracking algorithm. Therefore, the atomic algorithm can accurately decompose the components of the signal and has a good signal reconstruction ability.

TABLE 1: Decomposed parameters of voltage sag.

Atom numbers	A_q (V)	ρ_q	f_q (Hz)	ϕ_q (rad)	t_{sq} (s)	t_{eq} (s)
1	0.868	0.000	50	0.000	0.000	0.320
2	0.432	0.000	50	0.000	0.068	0.239
3	0.197	0.000	50	3.142	0.070	0.320
4	0.213	0.000	50	0.000	0.000	0.240

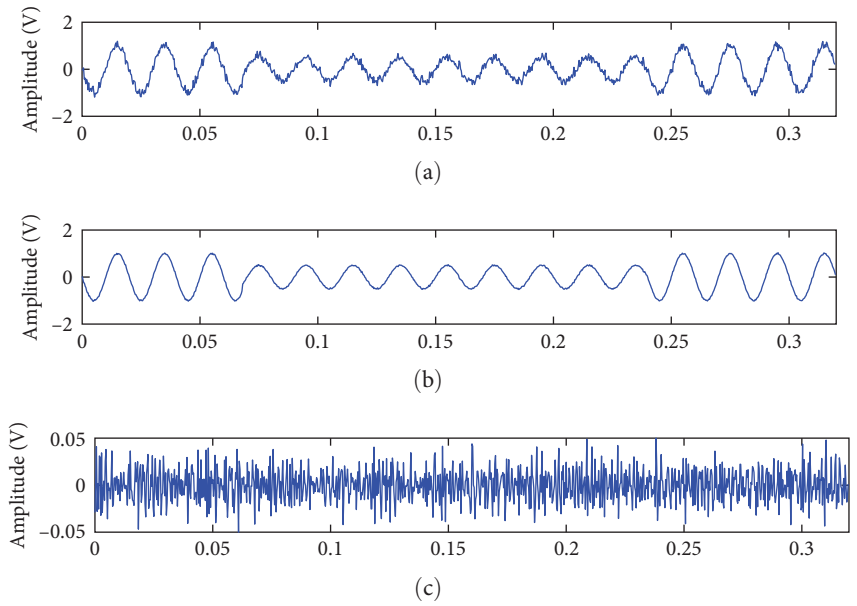

Figure 4: Decomposition results of IAD for voltage sag signal with 20 dB noise: (a) the original sag signal with SNR of 20 dB; (b) the reconstructed signal; (c) the residual component.

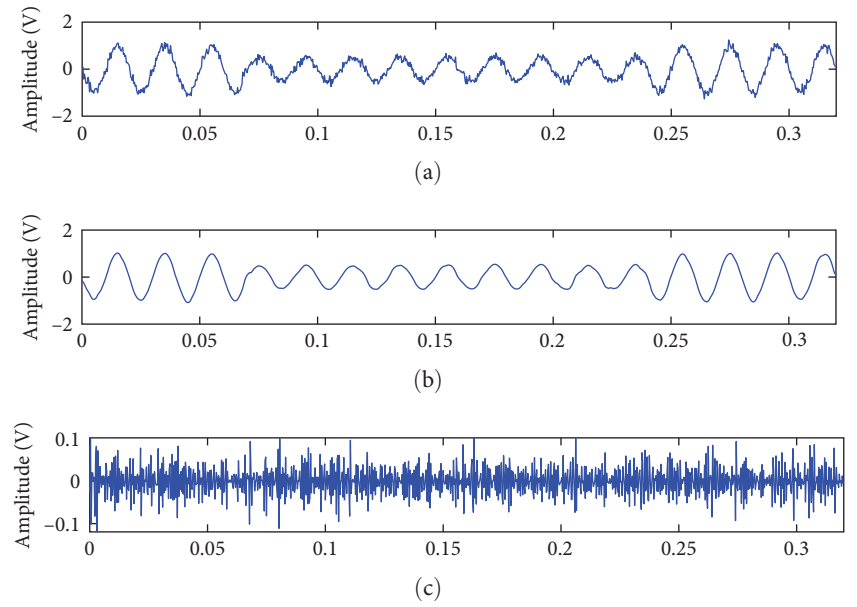

Figure 5: Decomposition results of WT for voltage sag signal with 20 dB noise: (a) the original sag signal with SNR of 20 dB; (b) the reconstructed signal; (c) the residual component.

Table 2: Evaluation indicators comparison for voltage sag signal.

Methods	SNR	E_m	N_{MSE}	N_{power}
IAD	Pure signal	1/43.5	0.0008	0.998
	30 dB	1/43.5	0.0008	0.999
	20 dB	1/43.5	0.0063	0.991
WT	Pure signal	1/13.1	0.0005	0.994
	30 dB	1/12.7	0.0011	0.991
	20 dB	1/12.5	0.0013	0.989

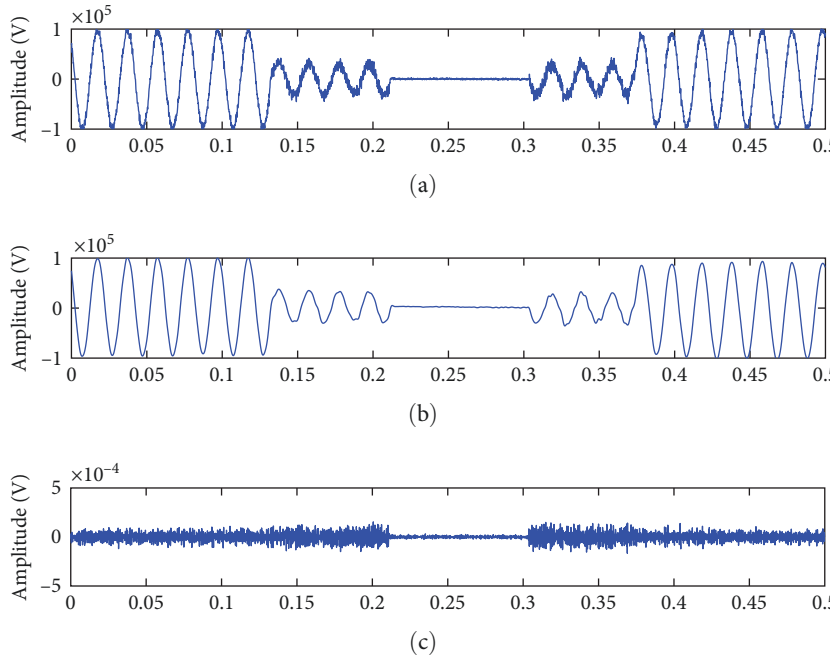

Figure 6: Decomposition results of IAD for combined voltage sag and momentary interruption signal: (a) the original signal; (b) the reconstruction signal after IAD; (c) the residual component of reconstruction.

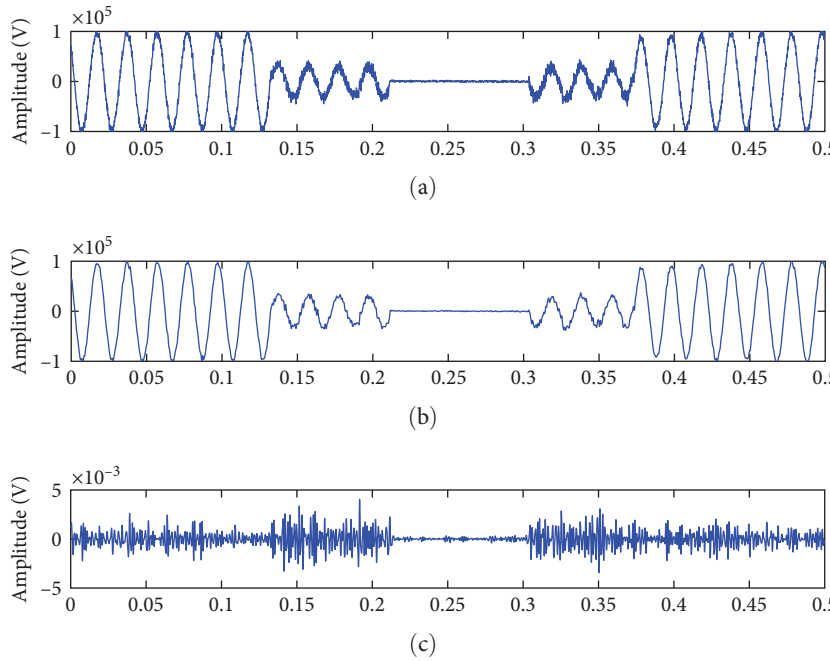

Figure 7: Decomposition results of WT for combined voltage sag and momentary interruption signal: (a) the original signal; (b) the reconstruction signal after WT decomposition; (c) the residual component of reconstruction.

To verify the performance of the proposed IAD method in a noisy environment, we added 20 dB Gaussian white noise to the above voltage sag signal, which was decomposed by the IAD method. The decomposition results are shown in Figure 4(a), which shows the original sag signal with 20 dB noise, which is decomposed and reconstructed to obtain the reconstructed signal, as shown in Figure 4(b). There is little difference between Figures 3(b) and 4(b), which shows that this method has good antinoise and signal reconstruction ability.

In addition, the WT method is used for comparison. The decomposition results are shown in Figure 5. The reconstructed signal by WT is shown in Figure 5(b), which describes that the waveform has some distortion compared with Figure 4(b). Meanwhile, the amplitude of the residual

Table 3: Evaluation indicators for combined sag and interruption signal with 20 and 30 dB noises.

Methods	SNR	E_m	N_{MSE}	N_{power}
IAD	Pure signal	1/29.7	0.0013	0.993
	30 dB	1/29.7	0.0015	0.990
	20 dB	1/29.7	0.0016	0.974
WT	Pure signal	1/13.4	0.0069	0.968
	30 dB	1/12.6	0.0087	0.956
	20 dB	1/12.2	0.0098	0.943

component is higher than that of the IAD method, as shown in Figure 4(c).

In order to compare the disturbance modeling performance of the proposed method, the evaluation indicators E_m, $N_{\mathrm{MSE}}, N_{\mathrm{power}}$ of IAD and WT are shown in Table 2. The results exhibit that the IAD has very high modeling efficiency E_m and the normalized mean-square error N_{MSE} and the energy ratio N_{power} are similar with WT.

4.2. Combined Signals with Voltage Sag and Momentary Interruption. The voltage sag and momentary interruption combined signal is generated by the electromagnetic transient program to simulate a short circuit fault, as shown in Figure 6(a). The combined signal was decomposed by the IAD method with five atomic iterations; the residual energy is very low, as shown in Figure 6(c). Figure 6(b) shows the reconstructed signal, which can accurately model the combined signal.

Similarly, the decomposition result of WT for the combined voltage sag and momentary interruption signal is shown in Figure 7. The reconstruction signal after WT decomposition still has some distortion in the sag waveform, as shown in Figure 7(b). In addition, the amplitude of the residual component is higher than that of the IAD method. This indicates that the disturbance signal modeling performance of WT is weaker than the IAD method proposed in this paper.

The performance of the proposed method is further reflected through the evaluation indicators E_m, N_{MSE}, N_{power}. Table 3 shows the indicators for combined signals with the IAD method and the WT. Similarly, the modeling efficiency E_m of IAD is higher than that of WT, and the normalized mean-square error N_{MSE} and the energy ratio N_{power} of IAD are also better than that of WT.

In addition, the IAD uses analytical parameters to represent the disturbance signals, which is independent of signal length and greatly improves the modeling efficiency. Furthermore, the atomic decomposition represents signals in a linear combination form, which is more suitable for different types of disturbance signals.

5. Conclusions

This paper proposed an IAD method for modeling voltage disturbances of the microgrids PCC. The proposed method can quickly and accurately quantify the voltage disturbance parameters, which can provide a basis for the voltage disturbance assessment and management in time. The coherent atom dictionary is constructed according to the characteristics of the PCC voltage disturbance of wind farms to improve the decomposition efficiency. In addition, an improved matching pursuit algorithm (IAD) is proposed to decrease computation quantities by alternating the search way of selecting the optimal atoms. Case studies showed that the proposed IAD method can achieve efficient and accurate modeling for voltage disturbances. Meanwhile, the evaluation indicators E_m, $N_{\mathrm{MSE}}, N_{\mathrm{power}}$ of IAD are better than that of WT.

The proposed measures in this paper, such as the damped sinusoidal atoms, the improved MP, and the subdictionaries, are designed specifically for PCC voltage disturbances modeling of microgrids to simplify the computations of atomic decomposition. However, the coherent atom dictionary is not over-complete, and it is necessary to further study how to construct the coherent atom dictionary of voltage fluctuation and flicker, so that it can be more widely used in various voltage disturbance problems caused by microgrid connections.

Data Availability

The data used to support the findings of this study are available from the corresponding author upon request.

Conflicts of Interest

The authors declare that they have no conflicts of interest.

Acknowledgments

This work is supported by the Science and Technology Project of State Grid Heilongjiang Electric Power Co., Ltd. in 2023 (522437230003).

References

[1] S. He, W. Tian, J. Zhang, K. Li, M. Zhang, and R. Zhu, "A high efficient approach for power disturbance waveform compression in the view of Heisenberg uncertainty," *IEEE Transactions on Industrial Informatics*, vol. 15, no. 5, pp. 2580–2591, 2019.

[2] J. O. Odhiambo, "Deep learning incorporated Bühlmann credibility in the modified Lee–Carter mortality model," *Mathematical Problems in Engineering*, vol. 2023, Article ID 8543909, 8 pages, 2023.

[3] J. Odhiambo, P. Ngare, and P. Weke, "Bühlmann credibility approach to systematic mortality risk modelling for sub-Saharan Africa populations (Kenya)," *Research in Mathematics*, vol. 9, no. 1, Article ID 2023979, 2022.

[4] J. Odhiambo, P. Weke, P. Ngare, R. Naryongo, and S. Sewe, "Poisson incorporated credibility regression modelling of systematic mortality risk for populations with finite data," *Mathematical Problems in Engineering*, vol. 2022, Article ID 1753542, 14 pages, 2022.

[5] G. S. Chawda, A. G. Shaik, M. Shaik et al., "Comprehensive review on detection and classification of power quality disturbances in utility grid with renewable energy penetration," *IEEE Access*, vol. 8, pp. 146807–146830, 2020.

[6] J. Wang, Z. Xu, and Y. Che, "Power quality disturbance classification based on compressed sensing and deep convolution neural networks," *IEEE Access*, vol. 7, pp. 78336–78346, 2019.

[7] E. B. Kapisch, V. V. de Morais, L. R. M. Silva, L. M. A. Filho, and C. A. Duque, "Spectral variation-based signal compression technique for gapless power quality waveform recording in smart grids," *IEEE Transactions on Industrial Informatics*, vol. 18, no. 7, pp. 4488–4498, 2022.

[8] C. Chen, W. Wang, H. Yin, L. Zhan, and Y. Liu, "Real-time lossless compression for ultrahigh-density synchrophasor and point-on-wave data," *IEEE Transactions on Industrial Electronics*, vol. 69, no. 2, pp. 2012–2021, 2022.

[9] R. Pourramezan, R. Hassani, H. Karimi, M. Paolone, and J. Mahseredjian, "A real-time synchrophasor data compression method using singular value decomposition," *IEEE Transactions on Smart Grid*, vol. 13, no. 1, pp. 564–575, 2022.

[10] L. Yan, J. Han, R. Xu, and Z. Li, "Model-free lossless data compression for real-time low-latency transmission in smart grids," *IEEE Transactions on Smart Grid*, vol. 12, no. 3, pp. 2601–2610, 2021.

[11] X. Chen, Y. Yang, Z. Cui, and J. Shen, "Wavelet denoising for the vibration signals of wind turbines based on variational mode decomposition and multiscale permutation entropy," *IEEE Access*, vol. 8, pp. 40347–40356, 2020.

[12] S. Turizo, G. Ramos, and D. Celeita, "Voltage sags characterization using fault analysis and deep convolutional neural networks," *IEEE Transactions on Industry Applications*, vol. 58, no. 3, pp. 3333–3341, 2022.

[13] Y. Yu, W. Zhao, S. Li, and S. Huang, "A two-stage wavelet decomposition method for instantaneous power quality indices estimation considering interharmonics and transient disturbances," *IEEE Transactions on Instrumentation and Measurement*, vol. 70, pp. 1–13, 2021.

[14] W. Hao, B. Hu, and L. Zhao, "Compression of power quality disturbance using wavelet-atomic decomposition for grid-connected wind farms," in *2023 6th International Conference on Electrical Engineering and Green Energy (CEEGE)*, pp. 171–178, IEEE, Grimstad, Norway, June 2023.

[15] X. Zheng, Y. Y. Tang, and J. Zhou, "A framework of adaptive multiscale wavelet decomposition for signals on undirected graphs," *IEEE Transactions on Signal Processing*, vol. 67, no. 7, pp. 1696–1711, 2019.

[16] Z. Feng, Y. Zhou, M. J. Zuo, F. Chu, and X. Chen, "Atomic decomposition and sparse representation for complex signal analysis in machinery fault diagnosis: a review with examples," *Measurement*, vol. 103, pp. 106–132, 2017.

[17] M. P. Tcheou, L. Lovisolo, E. A. B. da Silva, M. A. M. Rodrigues, and P. S. R. Diniz, "Optimum rate-distortion dictionary selection for compression of atomic decompositions of electric disturbance signals," *IEEE Signal Processing Letters*, vol. 14, no. 2, pp. 81–84, 2007.

[18] W. Gao, R.-J. Wai, Y.-F. Liao, M.-F. Guo, and Y. Yang, "Internal overvoltage identification of distribution network via time-frequency atomic decomposition," *IEEE Access*, vol. 7, pp. 85110–85122, 2019.

[19] Y. Han, Y. Feng, P. Yang, L. Xu, and A. S. Zalhaf, "An efficient algorithm for atomic decomposition of power quality disturbance signals using convolutional neural network," *Electric Power Systems Research*, vol. 206, Article ID 107790, 2022.

[20] X. Zhang, Z. Liu, L. Wang, J. Zhang, and W. Han, "Bearing fault diagnosis based on sparse representations using an improved OMP with adaptive Gabor sub-dictionaries," *ISA Transactions*, vol. 106, pp. 355–366, 2020.

[21] A. Agarwal, A. Anandkumar, and P. Netrapalli, "A clustering approach to learning sparsely used overcomplete dictionaries," *IEEE Transactions on Information Theory*, vol. 63, no. 1, pp. 575–592, 2017.

[22] L. Lovisolo, E. A. B. da Silva, M. A. M. Rodrigues, and P. S. R. Diniz, "Efficient coherent adaptive representations of monitored electric signals in power systems using damped sinusoids," *IEEE Transactions on Signal Processing*, vol. 53, no. 10, pp. 3831–3846, 2005.